

1 BIOLOGICAL SCIENCES: Cell Biology

2

3 **Circadian Proteins Cry and Rev-erb Deepen Cellular Quiescence**  
4 **by Down-regulating Cyclin D and Cdk4,6**

5

6 Xia Wang<sup>1#</sup>, Bi Liu<sup>1,2#</sup>, Qiong Pan<sup>1</sup>, Jungeun Sarah Kwon<sup>1</sup>, Matthew A. Miller<sup>1</sup>,  
7 Kimiko Della Croce<sup>1</sup>, Guang Yao<sup>1,3\*</sup>

8

9 <sup>1</sup>Department of Molecular and Cellular Biology, University of Arizona, Tucson, AZ,  
10 85721, USA

11 <sup>2</sup>School of Life Sciences, Westlake University, Hangzhou, 310024, China

12 <sup>3</sup>Arizona Cancer Center, University of Arizona, Tucson, AZ, 85719, USA

13

14

15 <sup>#</sup>These authors contributed equally to this work.

16 <sup>\*</sup>Correspondence should be addressed to: [guangyao@arizona.edu](mailto:guangyao@arizona.edu)

17

18      **ABSTRACT**

19      The proper balance and transition between cellular quiescence and proliferation are  
20      critical to tissue homeostasis, and their deregulations are commonly found in many  
21      human diseases, including cancer and aging. Recent studies showed that the reentry of  
22      quiescent cells to the cell cycle is subjected to circadian regulation. However, the  
23      underlying mechanisms are largely unknown. Here, we report that two circadian  
24      proteins, Cryptochrome (Cry) and Rev-erb, deepen cellular quiescence in rat embryonic  
25      fibroblasts, resulting in stronger serum stimulation required for cells to exit quiescence  
26      and reenter the cell cycle. This finding was opposite from what we expected from the  
27      literature. By modeling a library of possible regulatory topologies linking Cry and Rev-  
28      erb to a bistable Rb-E2f gene network switch that controls the quiescence-to-  
29      proliferation transition and by experimentally testing model predictions, we found Cry  
30      and Rev-erb converge to downregulate Cyclin D/Cdk4,6 activity, leading to an  
31      ultrasensitive increase of the serum threshold to activate the Rb-E2f bistable switch.  
32      Our findings suggest a mechanistic role of circadian proteins in modulating the depth  
33      of cellular quiescence, which may have implications in the varying potentials of tissue  
34      repair and regeneration at different times of the day.

35

36      **Keywords:** Circadian; Quiescence; Dormancy; Proliferation; Quiescence depth;

37      Cell cycle entry; Rb-E2f switch; Exploratory model search

38

39

40 **Significance Statement:** Tissue homeostasis requires a proper balance between  
41 quiescence and proliferation. The quiescence-to-proliferation transition appears  
42 affected by the circadian clock: the rates to activate stem and progenitor cells to  
43 proliferate can vary diurnally. But the underlying molecular mechanisms are largely  
44 unknown. Here we show increasing circadian proteins Cry and Rev-erb pushed cells to  
45 deeper quiescence and become harder to transition into proliferation. Through  
46 exploratory model searches and experimental tests, we found Cry and Rev-erb converge  
47 to downregulate Cyclin D/Cdk4,6, which increases the activation threshold of a bistable  
48 Rb-E2f gene switch underlying quiescence exit. Our findings suggest novel and  
49 converging mechanistic roles of circadian proteins in regulating cellular quiescence  
50 depth and potentially varying abilities for tissue regeneration around the circadian clock.

51

## 52 INTRODUCTION

53 Upon growth signals, various types of quiescent cells (e.g., adult stem and progenitor  
54 cells) can reenter the cell cycle to proliferate. This quiescence-to-proliferation transition  
55 is fundamental to tissue homeostasis and repair [1-3]. This transition, as shown in recent  
56 studies, also appears to be affected by the circadian clock. For example, quiescent  
57 neural stem cells and progenitor cells initiate neurogenesis to produce new neurons in  
58 a circadian-dependent manner [4, 5]; similarly does the circadian activation of hair  
59 follicle stem cells for tissue renewal [6].

60 Circadian clocks are present in cells throughout mammalian tissues. These  
61 clocks are cell-autonomous yet orchestrated by a master pacemaker in the  
62 hypothalamus [7-10]. Cellular circadian clocks are primarily driven by coupled  
63 negative feedback loops formed between a Bmal1/Clock heterodimer and its  
64 transcriptional targets: cryptochrome (Cry), period (Per), and Rev-erb, which in turn  
65 inhibit Bmal1/Clock [11]. In proliferating cells, several circadian proteins crosstalk to  
66 cell cycle proteins [12-15]. For example, Bmal1 represses the expression of Myc [16,  
67 17], a transcription factor that promotes cell proliferation; Rev-erb represses the  
68 expression of p21<sup>Cip1</sup> (p21 for short) [18], a cyclin-dependent kinase (Cdk) inhibitor of  
69 G1 and S Cdk (Cdk4,6 and Cdk2); Bmal1/Clock activates Wee1 [19], leading to the  
70 suppression of Cyclin B1/Cdk1 activity that is critical to mitosis, while Cry does the  
71 opposite by inhibiting Wee1 [19]. These molecular interactions lead to the circadian

72 regulation of the proliferative cell cycle [17-20]. However, how the circadian clock  
73 regulates the transition to proliferation from quiescence remains largely unknown.

74 Cellular quiescence is not a homogeneous state but heterogeneous [1, 21, 22].  
75 The likelihood of quiescence-to-proliferation transition is reversely correlated with  
76 quiescence depth. Upon growth stimulation, cells at deeper quiescence are less likely  
77 to, and take longer time if they do, reenter the cell cycle and initiate DNA replication  
78 than cells at shallower quiescence [21, 23, 24]. Deeper quiescence is often observed in  
79 aging cells in the body [25, 26] or in cells remaining quiescent for longer durations in  
80 culture [21, 27]. Shallower quiescence is seen in stem cells responding to tissue injury  
81 [28, 29] or related systemic signals [30, 31].

82 We have shown recently that quiescence depth is regulated by an Rb-E2f  
83 bistable switch and its interacting pathways [21, 32, 33]. E2f transcription activators  
84 (E2f1-3a, referred to as E2f for short), by transactivating genes necessary for DNA  
85 synthesis and cell cycle progression, are both necessary and sufficient for cell cycle  
86 entry from quiescence [34, 35]. E2f is repressed by Rb family proteins (referred to as  
87 Rb for short) in quiescent cells and activated upon stimulation with serum growth  
88 factors. E2f activation upon serum stimulation is mediated by multiple positive  
89 feedbacks leading to the phosphorylation and inhibition of Rb by Cyclin D  
90 (CycD)/Cdk4,6 and Cyclin E (CycE)/Cdk2 complexes. These integrated positive  
91 feedbacks establish the bistability at the Rb-E2f gene network level, converting graded  
92 and transient growth signals into an all-or-none E2f activation [32, 36], which further  
93 triggers and couples with APC/C<sup>CDH1</sup> inactivation via EMI1 and CycE/Cdk2, leading  
94 to an irreversible entry of the S-phase of the cell cycle and thus the quiescence-to-  
95 proliferation transition [37, 38]. The serum threshold (i.e., minimum serum  
96 concentration) that activates the Rb-E2f bistable switch, the E2f-activation threshold  
97 for short, has been shown to determine quiescence depth [21].

98 In this study, we examined the effects of two circadian proteins, Cry and Rev-  
99 erb, on the cellular transition from quiescence to proliferation. We anticipated that Cry  
100 and Rev-erb activities, via their known roles in upregulating Myc and downregulating  
101 p21, respectively, might lead to shallower quiescence by reducing the E2f-activation  
102 threshold [21]. However, we observed the opposite in our experiments. Through a  
103 comprehensive modeling search and follow-up experiments, we found both Cry and  
104 Rev-erb play novel roles that converge to downregulate CycD/Cdk4,6 activity, leading

105 to an ultrasensitive increase of the E2f-activation threshold and quiescence depth.

106

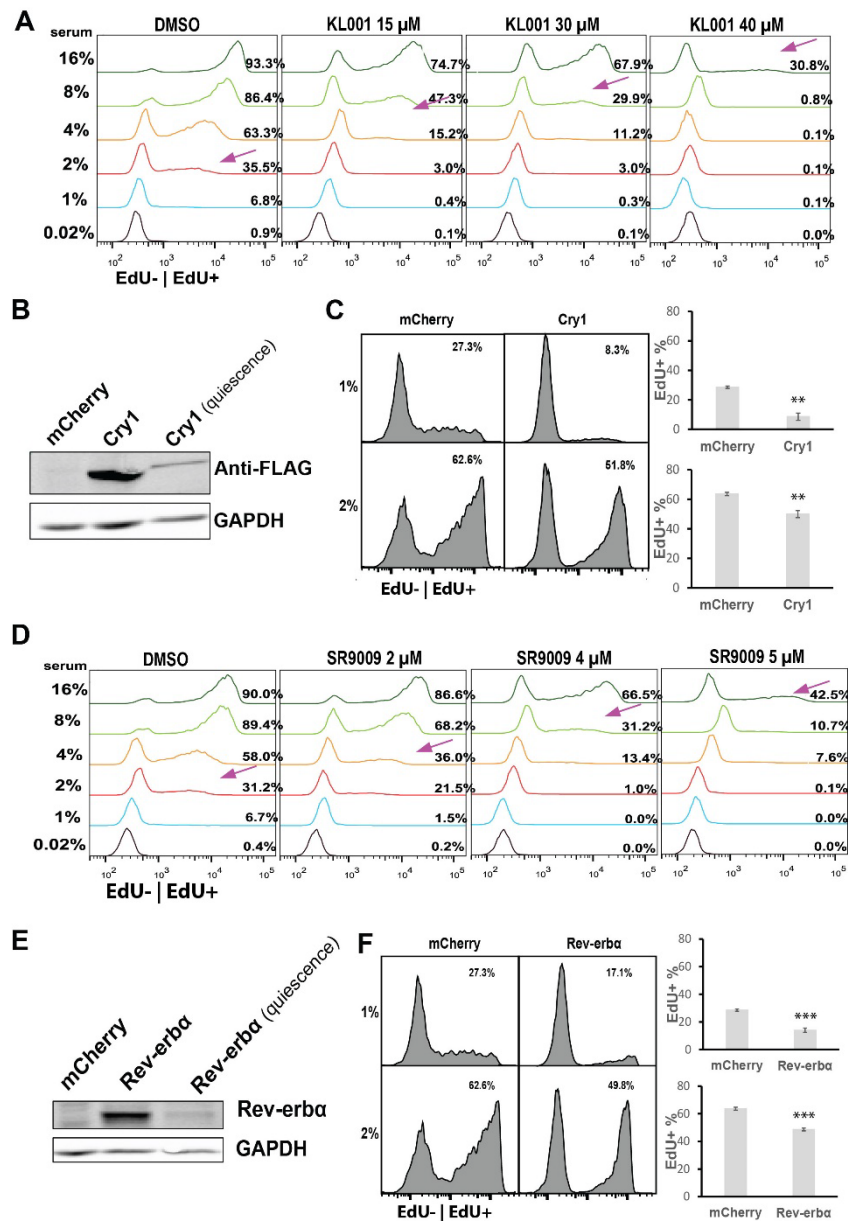
## 107 **RESULTS**

### 108 **Circadian protein Cry deepens cellular quiescence**

109 Earlier studies have suggested that Bmal1 inhibits Myc expression, and consistently,  
110 Cry upregulates Myc [16, 17]. As Myc promotes E2f activation [39], we tested the  
111 potential effect of Cry on the quiescence-to-proliferation transition. We started by  
112 applying a recently developed specific Cry agonist KL001 [40] to rat embryonic  
113 fibroblasts (REF/E23 cells). When treated with KL001 ( $\leq 40 \mu\text{M}$ , below its cytotoxicity  
114 level, Fig S1A), REF/E23 cells induced to quiescence by serum starvation did exhibit  
115 a modest but statistically significant increase of Myc protein (Fig. S2A); this increase,  
116 however, became insignificant when quiescent REF/E23 cells were stimulated to enter  
117 the cell cycle (10 and 14 hours after serum stimulation, Fig. S2B). Assuming the modest  
118 increase of Myc in quiescent cells might facilitate their E2f activation and transition  
119 into proliferation, we expected quiescence depth might be slightly reduced, if any, under  
120 KL001 treatment. To our surprise, we found KL001 treatment deepened quiescence:  
121 with increasing KL001 doses, increasing serum concentrations were needed to drive  
122 similar percentages of cells to reenter the cell cycle (arrow pointed,  $\sim 45\%$ ; Fig. 1A,  
123 based on EdU incorporation, EdU+; Fig. S2C, based on the “On”-state of an E2f-GFP  
124 reporter, E2f-ON [32]). Consistently, when stimulated at a given serum concentration  
125 (e.g., 8% serum, Fig. 1A and S2C), the percentage of cells that reentered the cell cycle  
126 decreased with increasing KL001 doses.

127 Similarly, quiescence deepened with the treatment of a different Cry agonist or  
128 with ectopic Cry1 expression. First, when REF/E23 cells were treated with the 2<sup>nd</sup> Cry  
129 agonist, KL002, increasing serum concentrations were needed to drive similar  
130 percentages of cells to reenter the cell cycle (Fig. S2D, based on EdU+%; Fig. S2E,  
131 based on E2f-ON%). Consistently, when stimulated at a given serum concentration, the  
132 percentage of cells that reentered the cell cycle decreased with increasing KL002 doses  
133 (Fig. S2 D and E). Second, in quiescent REF/E23 cells transfected with a Cry1 vector  
134 and expressing ectopic Cry1 (albeit at a much lower level in quiescence than in growing  
135 condition, Fig. 1B), the percentage of cells that reentered the cell cycle (EdU+%) in  
136 response to serum stimulation decreased ( $p < 0.01$ ) compared to that in the mCherry-

137 transfection control (driven by the same CMV promoter, Fig. 1C). Our results from two  
 138 Cry agonists and ectopic Cry expression, put together, suggested that Cry drove cells  
 139 to deeper quiescence, instead of facilitating the quiescence-to-proliferation transition.  
 140



141

142 **Figure 1. Cry and Rev-erb drive cells to deeper quiescence.**

143 (A) Effect of Cry agonist KL001 on quiescence depth. REF/E23 cells were first induced to  
 144 quiescence by serum starvation for 2 days, then treated with the agonist at the indicated  
 145 concentrations in starvation medium for 1 day; cells were subsequently stimulated by switching to  
 146 growth medium containing serum and agonist at the indicated concentrations for the indicated  
 147 durations. This protocol, serum stimulation (STI) of 3-day quiescent cells under agonist treatment  
 148 (STI.3dq/agonist for short), was used for all agonist-related tests in this study unless otherwise noted.  
 149 Indicated to the right of individual histograms are the percentages of cells becoming EdU+ after 24  
 150 hours of serum stimulation. Arrows indicate the approximate serum concentrations resulting in  
 151 EdU+% = 45%.

152 (B) Ectopic Cry1 expression. Proliferating cells were transfected with a FLAG-tagged Cry1 vector  
153 or a mCherry control and then subjected to Western blot with a FLAG antibody. “Quiescence”  
154 indicates the Western blot performed in Cry1-transfected cells induced to quiescence by 2-day  
155 serum-starvation.

156 (C) Effect of ectopic Cry1 on quiescence depth. Cry1- or mCherry-transfected cells were induced  
157 to quiescence by 2-day serum-starvation, stimulated with serum at the indicated concentrations for  
158 30 hours, and assayed for EdU+%. Error bar, SEM (n = 3). \*\*p < 0.01, \*\*\*p < 0.001 (1-tailed t-test;  
159 the same below).

160 (D) Effect of Rev-erb agonist SR9009 on quiescence depth. Quiescent cells were serum stimulated  
161 following the STI.3dq/agonist protocol. Serum and SR9009 concentrations are as indicated. EdU+%  
162 at the 24-hour after serum stimulation are shown to the right of individual histograms. Arrows  
163 indicate the approximate serum concentrations leading to EdU+% = 45%.

164 (E) Ectopic Rev-erb $\alpha$  expression. Proliferating cells were transfected with a Rev-erb $\alpha$  vector or a  
165 mCherry control and then subjected to Western blot with a Rev-erb antibody. “Quiescence” indicates  
166 the Western blot performed in Rev-erb-transfected cells induced to quiescence by 2-day serum-  
167 starvation.

168 (F) Effect of ectopic Rev-erb on quiescence depth. Rev-erb- or mCherry-transfected cells were  
169 induced to quiescence by 2-day serum-starvation, stimulated with serum at the indicated  
170 concentrations for 30 hours, and assayed for EdU+%. Error bar, SEM (n = 3). \*\*p < 0.01.

171

## 172 **Circadian protein Rev-erb deepens cellular quiescence**

173 Next, we examined another link between circadian proteins and the Rb-E2f switch:  
174 Rev-erb inhibits the expression of Cdk inhibitor (CKI) p21 [18], while p21 was known  
175 to deepen quiescence by increasing the E2f-activation threshold [21]. Therefore, we  
176 expected Rev-erb to reduce the E2f-activation threshold and thus quiescence depth.  
177 When we treated REF/E23 cells with a Rev-erb agonist SR9009 ( $\leq 5 \mu\text{M}$ , below its  
178 cytotoxicity level, Fig S1B), we did observe a significant decrease of p21 protein level  
179 at intermediate and high SR9009 doses (4 and 5  $\mu\text{M}$ ) both in quiescence (Fig. S3A) and  
180 during cell cycle entry (10 and 14 hours after serum stimulation, Fig. S3B). However,  
181 SR9009-treated cells did not move to shallower quiescence but deeper: with increasing  
182 SR9009 doses, increasing serum concentrations were needed to drive similar  
183 percentages of cells to reenter the cell cycle (arrow pointed,  $\sim 45\%$ ; Fig. 1D, based on  
184 EdU+%; Fig. S3C, based on E2f-ON%). When stimulated with serum at a given  
185 concentration, the percentage of cells that reentered the cell cycle decreased with  
186 increasing SR9009 doses (Fig. 1D and Fig. S3C). Similarly, treating cells with the 2<sup>nd</sup>  
187 Rev-erb agonist, SR9011, also deepened quiescence (Fig. S3D and E). Consistent with  
188 the effects of Rev-erb agonists, ectopic Rev-erb expression deepened quiescence: in  
189 quiescent REF/E23 cells transfected with a Rev-erb vector and expressing ectopic Rev-  
190 erb (albeit at a much lower level in quiescence than in growing condition, Fig. 1E), the  
191 percentage of cells that reentered the cell cycle (EdU+%) in response to serum  
192 stimulation decreased (p < 0.01) compared to that in the mCherry-transfection control



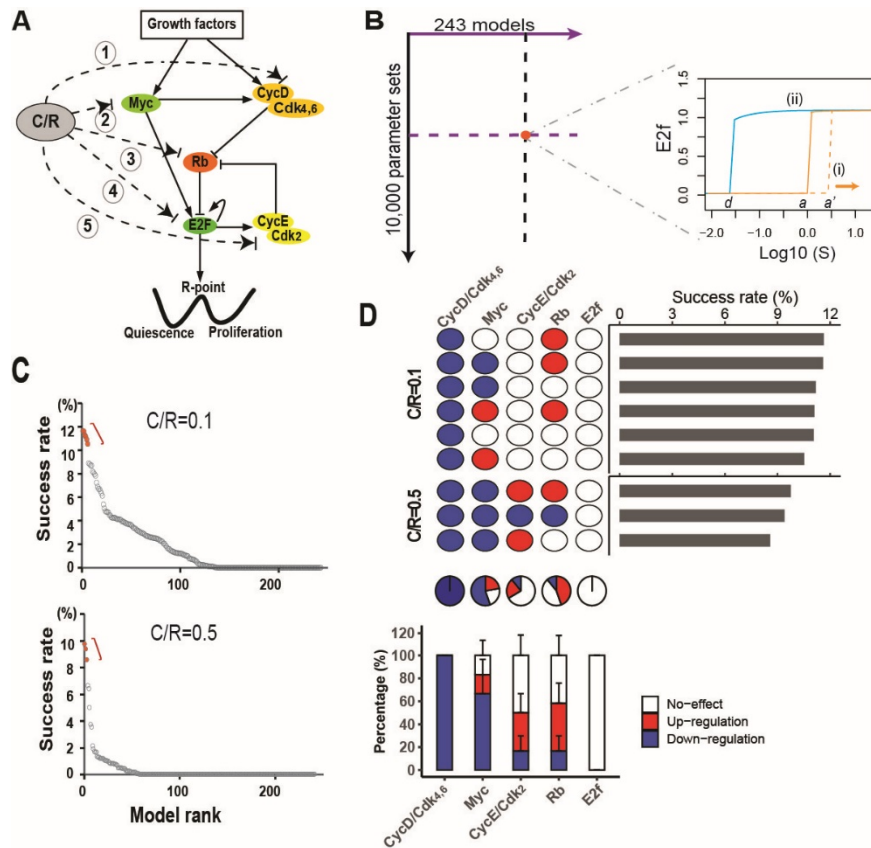
193 (driven by the same CMV promoter, Fig. 1F). Combining our results based on two  
194 agonists and ectopic expression, it suggested that Rev-erb drove cells to deeper  
195 quiescence instead of facilitating the quiescence-to-proliferation transition.

196  
197 **Both Cry and Rev-erb downregulate CycD/Cdk4,6 to deepen quiescence as**  
198 **predicted by exploratory model search**

199 Circadian proteins Cry and Rev-erb both deepened quiescence unexpectedly, indicating  
200 certain mechanistic links were missing in our understanding between these circadian  
201 proteins and cellular quiescence. As our earlier studies showed that the E2f-activation  
202 threshold determines quiescence depth [21, 36], this threshold mechanism provides a  
203 likely target for circadian regulation. We therefore searched for the potential missing  
204 links connecting Cry and Rev-erb to the E2f-activation threshold.

205 The Rb-E2f gene network is a complex system comprised of over 90 gene nodes  
206 involved in intertwined transcriptional controls and signaling cascades [41-45]. It  
207 would be time- and labor-intensive to test the candidate links one by one in experiments  
208 without first effectively narrowing down the candidates. To this end, we took advantage  
209 of our previously established mathematical model of the Rb-E2f bistable switch [32]  
210 and used computer simulation to predict the most likely missing link(s) responsible for  
211 the quiescence-deepening effects of Cry and Rev-erb. Our previous Rb-E2f bistable  
212 switch model considered five coarse-grained network modules: Myc, CycD/Cdk4,6, Rb,  
213 E2f, and CycE/Cdk2 (Fig. 2A). Upon serum growth signals, Myc and CycD/Cdk4,6 are  
214 upregulated. Myc promotes E2f expression; CycD/Cdk4,6 phosphorylates Rb and  
215 partially de-represses E2f. E2f activates CycE/Cdk2, which further phosphorylates Rb  
216 and de-repress E2f, forming a positive feedback loop. E2f transactivates its own  
217 expression, forming another positive feedback loop that reinforces E2f activation. Next,  
218 we considered Cry or Rev-erb (the C/R module, Fig. 2A) might directly or indirectly  
219 interact with any or all of the five modules (i.e., five possible links), and exert one of  
220 three net effects (up-regulation, down-regulation, or no effect). For example, the two  
221 literature links we started the study with, Cry upregulating Myc and Rev-erb inhibiting  
222 p21, were reflected in C/R upregulating Myc and Cyclin/Cdk modules (CycD/Cdk4,6  
223 and CycE/Cdk2, via downregulating p21), respectively. Considering the possible  
224 combinations of 5 links with 3 effects each,  $3^5 = 243$  different topologies could be  
225 generated to connect C/R to the Rb-E2f switch.





226

227 **Figure 2. Modeling search for the missing links of how Cry and Rev-erb deepen quiescence.**

228 (A) Cry or Rev-erb (C/R) may crosstalk with any or all of the five Rb-E2f network modules, and  
 229 each of the five links (1-5) can have one of the three possible net effects: upregulation,  
 230 downregulation, and no-effect, thus generating  $3^5 = 243$  possible network topologies.

231 (B) Model search and simulation. Each of the 243 models was simulated with 10,000 random  
 232 parameter sets; with each parameter set, the model was evaluated according to two criteria: (i) E2f-  
 233 activation threshold  $a' \geq 3$  (serum units); and (ii) bistability (as in the base model, E2f-activation  
 234 threshold  $a > \text{E2f-deactivation threshold } d$ ). S (x-axis), serum unit; E2f (y-axis), steady-state E2f  
 235 level. Solid orange and blue curves indicate E2f serum-responses in the base model simulated from  
 236 the quiescence and proliferation initial conditions, respectively. For simplicity, only the E2f serum-  
 237 response from quiescence simulated with one random parameter set (dashed orange curve) is shown.  
 238 See Materials and methods for details.

239 (C) Model ranking. The 243 models were ranked from left to right (x-axis) based on model  
 240 success rate (y-axis), which indicated the percentage of events (random parameter sets) in which the  
 241 model simulation outcome fulfilled the two criteria (i) and (ii). Simulation results with the C/R input  
 242 level of 0.1 and 0.5 are shown at the top and bottom, respectively.

243 (D) Link features of top-ranked models. (Top) Highest-ranked models with similar success rates at  
 244 C/R = 0.1 and 0.5, respectively (red dots in C). The link features in each model are shown according  
 245 to the upregulation (red), downregulation (blue), or no-effect (white) of the indicated target node by  
 246 C/R. (Middle) Pie chart of the percentage of each link feature at the indicated target node among  
 247 the combined 9 models (top). (Bottom) The average percentage of each link feature at the indicated  
 248 target node between the two model groups (C/R = 0.1 and 0.5, respectively, top). Error bar, SD.  
 249

250 We constructed a library of 243 ordinary differential equation (ODE) models to  
 251 represent the 243 network topologies. Based on our experimental observations, we set  
 252 two search criteria for the most likely missing link(s) between C/R and the Rb-E2f  
 253 switch: (i) increasing the E2f-activation threshold, and (ii) maintaining the network

254 bistability. Specifically, for criterion i, we set the E2f-activation threshold to increase  
255 from 1.0 in the previous base model [32] to  $\geq 3.0$ , since comparable EdU+% was  
256 obtained with 1% serum in the DMSO control and  $\sim 3\%$  serum under KL001 and  
257 SR9009 treatments at intermediate doses (KL001, 30  $\mu\text{M}$ ; SR9009, 4  $\mu\text{M}$ ; Fig. 1A and  
258 D). Criterion ii was set because we expected the Rb-E2f bistable switch to remain  
259 critical to the proper quiescence-to-proliferation transition under circadian regulation;  
260 it was also consistent with the bimodal E2f expression observed under KL001 and  
261 SR9009 treatments (similar to the DMSO control, Fig. S2C and S3C).

262 We subsequently simulated each of the 243 ODE models with a collection of  
263 random parameter sets. Each set contained 5 model parameters that dictated the  
264 strengths of the 5 links from C/R to Rb-E2f network modules ( $I_{1-5}$ , Tables S1 and S2),  
265 with parameter values simultaneously and randomly selected within the numerical  
266 ranges as determined in our previous modeling studies [32, 46]. We then calculated the  
267 success rate of each of the 243 models in fulfilling the search criteria (i) and (ii) across  
268 the random parameter sets (Fig. 2B, see Materials and Methods for detail). In this regard,  
269 we also applied two different C/R input levels to account for relatively low and high  
270 agonist doses, respectively (Fig. 2C). The models with the highest success rates (i.e.,  
271 most robust against parameter variations [46-48]) were considered the most likely  
272 explanations for how Cry and Rev-erb increased the E2f-activation threshold and  
273 deepened quiescence as we observed in experiments (Fig. 1A and D).

274 We found the compositions of the top 10 models remained the same after 5,000  
275 random parameter sets at  $C/R = 0.1$  (Table S3) and 3,750 parameter sets at  $C/R = 0.5$   
276 (Table S4), respectively, suggesting the model search results were stabilized. As seen  
277 in Fig. 2C, the final model success rates (after 10,000 parameter sets) declined rapidly  
278 moving away from the top-ranked models at each C/R input level, suggesting that a  
279 limited number of model topologies were viable for the C/R activity to deepen  
280 quiescence. That said, no single model “winner” stood out. For example, the top 6  
281 models at  $C/R = 0.1$  (red dots, Fig. 2C top panel) formed a cluster; within the cluster,  
282 any two neighboring models A and B exhibited similar success rates (s.r.), with the  
283 relative s.r. difference  $(s.r._A - s.r._B) / s.r._A < 10\%$ . The same was true for the top 3 models  
284 at  $C/R = 0.5$  (red dots, Fig 2C bottom). Comparing these top s.r. models (6 at  $C/R = 0.1$ ;  
285 3 at  $C/R = 0.5$ ), one uniquely shared feature became apparent: the downregulation of  
286 CycD/Cdk4,6 by C/R in every model (Fig. 2D). Alternatively, when we chose the 10

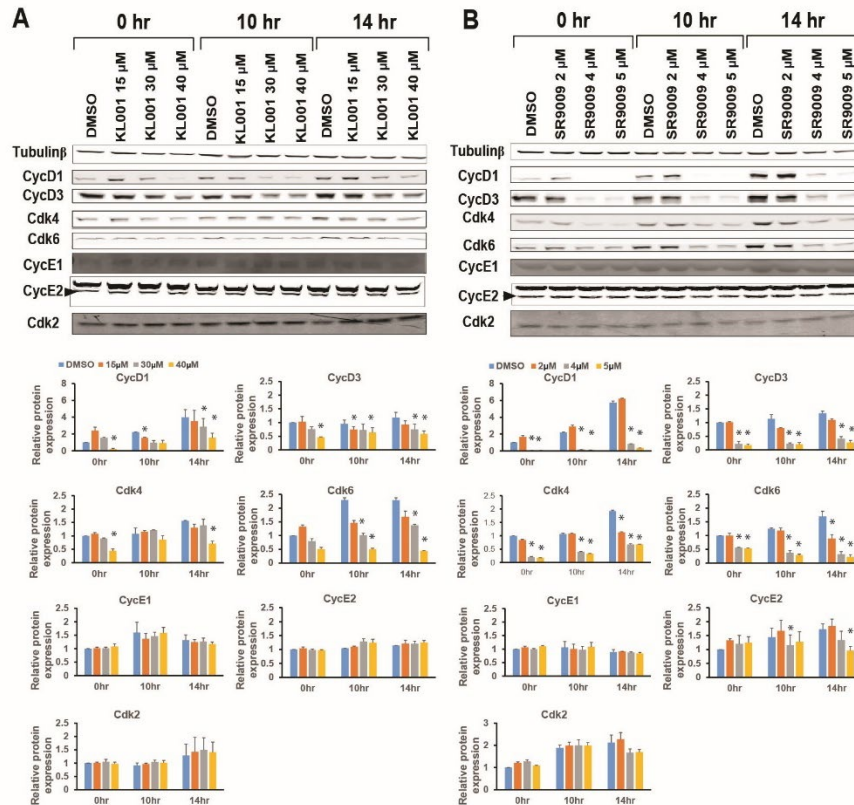
287 top-ranked models at each C/R input level (10 at C/R = 0.1; 10 at C/R = 0.5) as another  
288 high-s.r. model selection approach, CycD/Cdk4,6 downregulation by C/R was again the  
289 number one shared feature (Fig. S4). These model simulation results predicted that Cry  
290 and Rev-erb likely induced deep quiescence by primarily targeting and downregulating  
291 CycD/Cdk4,6 activity. We will further interpret these modeling results in Discussion.

### 292 **Experimental support for CycD/Cdk4,6 as the primary target of Cry and Rev-erb**

293 To test our model predictions, we measured the responses of CycD/Cdk4,6 complex  
294 components to Cry and Rev-erb and compared them to those of CycE/Cdk2 complex  
295 components. Specifically, following the same STI.3dq/agonist protocol (Fig. 1), we  
296 treated REF/E23 cells with Cry and Rev-erb agonists and measured the protein levels  
297 of D-type cyclins CycD1 and CycD3 (CycD2 is not expressed in REF/E23 cells [23]),  
298 Cdk4, and Cdk6, as well E-type cyclins (CycE1 and CycE2) and Cdk2 in quiescence  
299 and during cell cycle entry upon serum stimulation (Fig. 3).

300 We observed a significant downregulation of each tested CycD/Cdk4,6 complex  
301 component in response to both the Cry agonist KL001 (Fig. 3A) and Rev-erb agonist  
302 SR9009 (Fig. 3B). This general pattern occurred across the three tested time points (0,  
303 10, and 14 hours upon serum stimulation), especially at the medium and high agonist  
304 doses (KL001, 30 and 40  $\mu$ M; SR9009, 4 and 5  $\mu$ M; see Discussion for the low dose).  
305 This pattern of CycD/Cdk4,6 downregulation in response to Cry and Rev-erb agonists  
306 was in stark contrast to that of CycE/Cdk2 complex components, which exhibited non-  
307 significant changes overall (Fig. 3). These experimental observations were in good  
308 agreement with our model simulation results (Fig. 2D and S4), showing a convergent  
309 downregulation of CycD/Cdk4,6 by Cry and Rev-erb.

310 Similarly, we measured the responses of other proteins (Rb; Rb phosphatases  
311 PP1 and PP2A; Myc; CKIs p21, p27, and p16) in the Rb-E2f bistable switch network  
312 to Cry and Rev-erb agonists (Fig. S5). None of the observed responses, if any, would  
313 explain quiescence deepening (see Discussion). Put together, our experimental results  
314 supported the model-predicted unique role of CycD/Cdk4,6 as the convergent target of  
315 the circadian regulation by Cry and Rev-erb on quiescence depth.



316

317 **Figure 3. Cry and Rev-erb downregulate protein components of CycD/Cdk4,6 but not**  
 318 **CycE/Cdk2.**

319 The responses of individual protein components of CycD/Cdk4,6 and CycE/Cdk2 to the Cry agonist  
 320 KL001 (A) and Rev-erb agonist SR9009 (B) at the indicated doses were measured following the  
 321 STI.3dq/agonist protocol. Protein levels were measured by Western blot in quiescence (0 hr) and  
 322 during cell cycle entry (10 and 14 hr after stimulated with 4% serum) and normalized to the 0-hr  
 323 DMSO control. Error bar, SEM (n=2); \*p < 0.05 (1-tailed t-test).

324

325 **DISCUSSION**

326 The circadian clock aligns diverse cellular functions to periodic daily environmental  
 327 changes. In this study, we investigated the effects of two key circadian proteins, Cry  
 328 and Rev-erb, on cellular quiescence. We found upregulating Cry and Rev-erb drove  
 329 cells into deeper quiescence, opposite to what we had hypothesized based on literature.  
 330 To identify the missing links in our understanding, we evaluated an assembly of  
 331 potential network models and tested the converged predictions of the top-ranked models  
 332 experimentally. Our results suggested that both Cry and Rev-erb deepen quiescence by  
 333 primarily downregulating the CycD/Cdk4,6 complex components in the bistable Rb-  
 334 E2f gene network.

335 Why does the CycD/Cdk4,6 module play a unique role, targeted by both Cry  
 336 and Rev-erb, in mediating quiescence deepening? To move into deep quiescence, a cell

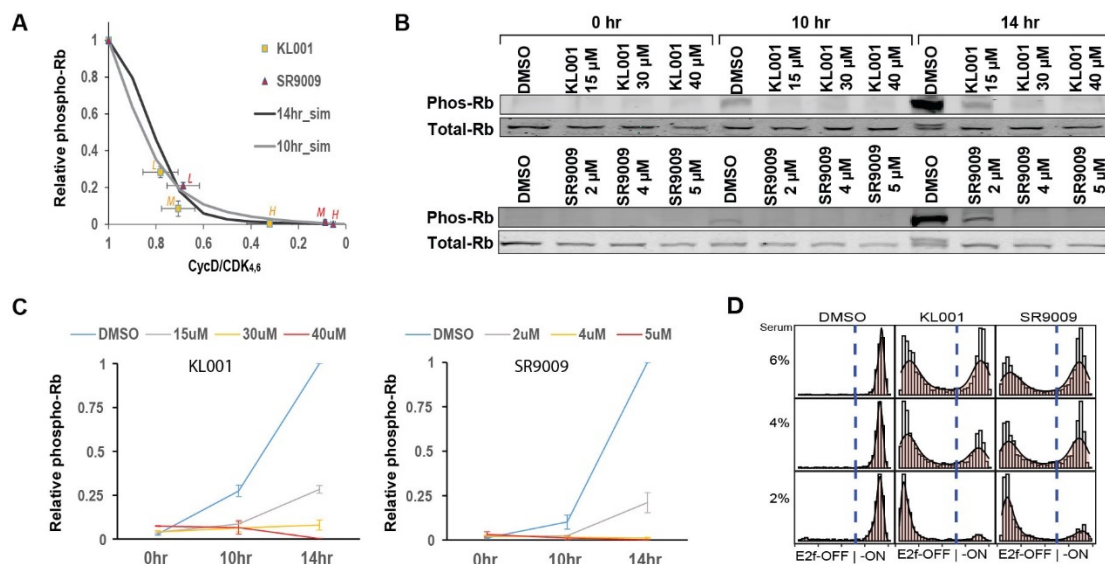
337 needs to increase its E2f-activation threshold while maintaining the Rb-E2f bistable  
338 switch for the proper quiescence-proliferation transition. In this regard, altering the  
339 activities of different Rb-E2f network modules has different consequences, depending  
340 on their positions and roles in the network (Fig. 2A). For example, changing Cyclin/Cdk  
341 activity has a stronger effect than changing Rb synthesis in increasing the E2f-  
342 activation threshold (determined by the ratio of unphosphorylated Rb over free E2f)  
343 [21]. Between the two G1 Cyclin/Cdks, late G1 CycE/Cdk2 hyper-phosphorylates Rb,  
344 and CycE/Cdk2 downregulation is associated with cell cycle arrest or exit into  
345 quiescence in proliferating cells [49, 50]. To drive quiescent cells deeper by targeting  
346 CycE/Cdk2, however, can be problematic. This is because downregulating CycE/Cdk2  
347 weakens the mutual-inhibition (i.e., positive feedback) loop between Rb and E2f that is  
348 essential to the network bistability [46] and consequentially the proper quiescence-to-  
349 proliferation transition. Similarly, targeting and inhibiting E2f to increase the E2f-  
350 activation threshold could be problematic, as repressing E2f weakens both positive  
351 feedbacks (Rb-E2f mutual-inhibition and E2f auto-activation) in the Rb-E2f network  
352 underlying the network bistability. By contrast, CycD/Cdk4,6 is upstream of and not  
353 directly involved in the positive feedback loops between Rb and E2F (Fig. 2A). We  
354 therefore expect that targeting to inhibit CycD/Cdk4,6 can better divide and conquer  
355 the needs to both increase the E2f-activation threshold and maintain the Rb-E2f bistable  
356 switch. Consistently, Cdk6 expression level was found to regulate the quiescence depth  
357 of human hematopoietic stem cells and impact their long-term preservation [51].

358 Relatedly, in proliferating cells, CycD level appears to reflect the protein  
359 synthesis rate of the mother cell, and the CycD level inherited from the mother cell is a  
360 key determinant of the proliferation-quiescence bifurcation of daughter cells [52, 53].  
361 On another note, a recent study suggested that CycD/Cdk4,6 mono-phosphorylates but  
362 does not inhibit Rb, and it meanwhile activates CycE/Cdk2 via an unidentified  
363 mechanism [54]. Although this new finding and the classic model differ in whether  
364 CycD/Cdk4,6 directly inhibits Rb, they are consistent in the role of CycD/Cdk4,6 in  
365 leading to CycE/Cdk2 activation and initiating the positive mutual-inhibition loop  
366 between Rb and E2f, which eventually leads to E2f activation and the passage of the  
367 restriction point during the quiescence-to-proliferation transition [55-60].

368 A closer look of CycD/Cdk4,6 responses to Cry and Rev-erb agonists showed  
369 that the protein levels of CycD1, CycD3, Cdk4, and Cdk6 decreased noticeably at the



370 medium and high doses of KL001 and SR9009, but not at their low doses (15  $\mu$ M  
 371 KL001, Fig. 3A; 2  $\mu$ M SR9009, Fig. 3B). How would this result at low dose conditions  
 372 explain the then still significantly deepened quiescence (Fig. 1A and D)? It turns out  
 373 Rb phosphorylation can be ultrasensitive to CycD/Cdk4,6 activity. That is, a small  
 374 downregulation of CycD/Cdk4,6 may cause a much larger decrease of Rb  
 375 phosphorylation during cell cycle entry (see the 10- and 14-hr sim curves, Fig. 4A), as  
 376 predicted by our Rb-E2f bistable switch model reflecting the phosphorylation-  
 377 dephosphorylation zero-order ultrasensitivity [61]. As a rough estimate, CycD/Cdk4,6  
 378 activity under the low doses of KL001 and SR9009 was reduced by about 30% during  
 379 cell cycle entry (considering joint cyclin, Cdk, and CKI levels, Table S5), which could  
 380 result in an over 80% reduction of Rb phosphorylation based on model simulations (Fig.  
 381 4A). We note that the estimate of CycD/Cdk4,6 was based on several assumptions  
 382 (Table S5) and may not be accurate. That said, our experimental observations of the  
 383 phospho-Rb level (S807/S811) across varying KL001 and SR9009 doses (low, medium,  
 384 and high, Fig. 4 B and C) were in good agreement with the model predictions  
 385 considering the estimated CycD/Cdk4,6 activities (Fig. 4A). This ultrasensitive  
 386 decrease of Rb phosphorylation increased the E2f-activation threshold and thus  
 387 deepened quiescence in our model, leading to noticeably fewer cells able to reenter the  
 388 cell cycle upon serum stimulation (Fig. 4D).



389

390 **Figure 4. Ultrasensitive effects of CycD/Cdk4,6 on Rb phosphorylation and quiescence depth.**  
 391 (A) Relationship between CycD/Cdk4,6 (x-axis) and relative phospho-Rb = (phosphorylated  
 392 Rb)/(total Rb) (y-axis). Model simulated results at the 10-hr (gray curve) and 14-hr (black curve)  
 393 after serum stimulation are shown together with experimentally estimated data points (CycD/Cdk4,6,  
 394 from Table S5; relative phospho-Rb, from C) under the treatments of KL001 (yellow squares) and  
 395 SR9009 (red triangles) at the low (L), medium (M), and high (H) doses, respectively.

396 (B) Effects of Cry and Rev-erb agonists (KL001, top; SR9009, bottom) on Rb phosphorylation.  
397 Quiescent cells were serum (4%) stimulated following the STI.3dq/agonist protocol in the presence  
398 of agonists at the indicated concentrations. The levels of phosphorylated Rb protein (S807/S811)  
399 were measured by Western blot at the 0-, 10-, and 14-hr time points after serum stimulation.  
400 (C) Quantification of the relative phospho-Rb in response to Cry and Rev-erb agonists (KL001, left;  
401 SR9009, right). Levels of phosphorylated Rb and total Rb were quantified from Western blots as in  
402 B. The relative phospho-Rb value of the 14-hr DMSO control is set to 1.0. Error bar, SD.  
403 (D) Stochastic simulations of quiescence exit under the low doses of KL001 (15  $\mu$ M) and SR9009  
404 (2  $\mu$ M). In each panel with the indicated condition, 1000 cells were simulated according to the  
405 relative Phospho-Rb level (14 hr) as in B, and the distribution of simulated E2f molecule numbers  
406 at the 24-hr after stimulation (4% serum) are shown (x-axis).

407

408           CycD/Cdk4,6 activity can be reduced by either downregulating CycD and  
409 Cdk4,6 or upregulating Cdk inhibitors (CKIs), including Cip/Kip proteins (most  
410 notably p21 and p27) and INK4 proteins (most notably p16). In REF/E23 cells treated  
411 with Cry and Rev-erb agonists, the p16 level did not change significantly while the  
412 levels of p21 and p27 mostly decreased but not increased (Fig. S5). These observations  
413 suggest that CKIs are not responsible for CycD/Cdk4,6 downregulation by Cry and  
414 Rev-erb. Since p16 is a marker of senescent cells, that it is not targeted and upregulated  
415 by circadian proteins in quiescent cells was anticipated. Yet, p21 and p27 could be  
416 viable options since they have been shown to drive deep quiescence in different  
417 contexts [21, 62]. We suspect that Cry and Rev-erb do not upregulate p21 and p27 to  
418 deepen quiescence is likely due to the specific regulatory mechanisms they employ to  
419 modulate the Rb-E2f bistable switch (see below).

420           Our modeling and experimental study here identified two novel connections  
421 from circadian proteins Cry and Rev-erb converging to downregulate CycD/Cdk4,6.  
422 The natures of these two newly discovered links remain unknown, such as how Cry and  
423 Rev-erb simultaneously downregulate multiple components (CycD1, CycD3, Cdk4 and  
424 Cdk6), and whether such regulations are direct or indirect. Similarly, we observed that  
425 both Cry and Rev-erb agonists reduced total Rb protein level (which would not deepen  
426 quiescence) but did not change the levels of Rb phosphatases PP1 and PP2A (Fig. S5).  
427 How both Cry and Rev-erb converge to similar regulatory patterns targeting a common  
428 subset of Rb-E2f network components are interesting questions that we hope to address  
429 in future studies.

430           As circadian proteins, Cry and Rev-erb levels fluctuate diurnally. Given  
431 upregulating Cry and Rev-erb deepened quiescence as observed in this study, we  
432 speculated that cellular quiescence depth might fluctuate diurnally too. Indeed, this is  
433 what we observed: circadian changes in the rate of quiescence-to-proliferation



434 transition in REF/E23 cells upon growth stimulation (Fig. S6). Further studies are  
435 needed to test and confirm which CycD/Cdk4,6 components fluctuate accordingly and  
436 are responsible for this phenomenon. Also, studies are needed to answer whether  
437 circadian fluctuation of quiescence depth occurs in various body tissues, resulting in  
438 different rates of tissue repair and regeneration at different times of the day. We also  
439 anticipate the differences of targeting CycD/Cdk4,6 and CycE/Cdk2 in regulating  
440 quiescence depth, as found in this study, may have implications in the applications of  
441 Cdk4,6 and Cdk2 inhibitors in clinical settings.

---

442 **MATERIALS AND METHODS**

443 **Cell culture, quiescence induction and exit**

444 Rat embryonic fibroblasts REF52/E23 cells stably harboring an E2f1 promoter-driven  
445 destabilized GFP reporter were derived previously as in [32]. Cells were routinely  
446 passed at a sub-confluent level and cultured in Dulbecco's Modified Eagle's Medium  
447 (DMEM) (No. 31053, Gibco, Thermo Fisher) with 10% of bovine growth serum (BGS,  
448 No. SH30541, Hyclone, GE Healthcare). To induce quiescence, growing cells were  
449 seeded at around  $10^5$  cells per well in 6-well culture plates (No. 353046, Corning  
450 Falcon), washed twice with DMEM, followed by culture in serum-starvation medium  
451 (0.02% BGS in DMEM) for 2 days or as indicated. To induce quiescence exit, serum-  
452 starvation medium was changed to serum-stimulation medium (DMEM containing  
453 serum at the indicated concentration), and cells were subsequently cultured for the  
454 indicated durations.

455 **Treatments of Cry and Rev-erb agonists**

456 Cry agonists KL001 (No. 233624, EMD Millipore) and KL002 (No. 13879, Cayman)  
457 and Rev-erb agonists SR9009 (No. 554726, Sigma-Aldrich) and SR9011 (No.  
458 SML2067, EMD Millipore) were applied by being included in serum starvation and  
459 stimulation media at the indicated times and concentrations. DMSO was used as a  
460 vehicle control.

461 **E2f activity and quiescence exit (EdU incorporation) Assays**

462 To measure E2f activity in individual cells, cells were harvested at the 24-hr time point  
463 after serum stimulation, fixed with 1% formaldehyde, and the fluorescence intensities  
464 of the E2f-GFP reporter in approximately 10,000 cells from each sample were measured  
465 using a LSR II flow cytometer (BD Bioscience). Flow cytometry data were analyzed  
466 using FlowJo software (v. 10.0). To assay for quiescence exit, EdU (2  $\mu$ M) was added  
467 to serum-stimulation medium, and cells were collected at the indicated time points,  
468 followed by Click-iT EdU assay according to the manufacturer's instruction.

469 **Ectopic expression**

470 Growing REF/E23 cells were kept at sub-confluence and transfected with pfmh-hCry1  
471 (a gift from Aziz Sancar; Addgene plasmid #25843) and pAdTrack-CMV FLAG Rev-  
472 erba expression vectors (a gift from Bert Vogelstein; Addgene plasmid #16405) for

473 ectopic expression of Cry1 and Rev-erb $\alpha$ , respectively, or with pCMV-mCherry (a gift  
474 from Lingchong You) as a control. Transfection was performed using Neon  
475 electroporation system (MPK5000, Invitrogen, Thermo Fisher) following the  
476 manufacturer's protocol. Briefly, in each transfection, about 10<sup>6</sup> cells were  
477 electroporated with 10  $\mu$ g of plasmid DNA at 1800 volts with two 20-millisecond pulses  
478 in a 100  $\mu$ l Neon tip.

#### 479 **Western blotting**

480 Cells were washed with DPBS once and then lysed in lysis buffer (50 mM Tris-HCl,  
481 pH 6.8, 2% sodium deoxycholate, 0.025% Bromophenol blue, 10% glycerol, 5%  $\beta$ -  
482 Mercaptoethanol). Extracted proteins were separated using SDS-PAGE and transferred  
483 onto nitrocellulose membranes. Immunoblot analyses were performed using antibodies  
484 against c-Myc (#sc-40), Rb (#sc-74562), Cyclin D1 (#sc-8396), Cyclin E2 (#sc-  
485 28351), Cdk2 (#sc-6248), Cdk4 (#sc-23896), p21 (#sc-53870), p27 (#sc-1641), PP1  
486 (#sc-7482), and PP2A (#sc-13600) from Santa Cruz; Phospho-Rb ( S807/S811;  
487 #9308T), Cyclin D3 (#2936T), Cyclin E1 (#20808), and Cdk6 (#3136T) from Cell  
488 Signaling; p16 (#ab51243) from Abcam; Tubulin beta (#MAB3408) from EMD  
489 Millipore Corp; and GAPDH (#MA5-15738-D680) from Invitrogen.

#### 490 **Model library generation and search**

491 Regulatory effects of Cry or Rev-erb ([CR] in Table S1) on a node  $x$  in the Rb-E2f  
492 network were modeled by adding  $m \cdot w \cdot [CR] / (1 + [CR])$  to the ODE  $d[x]/dt$  in our  
493 previously established Rb-E2f bistable switch model [19], with  $m = -1$  (negative  
494 regulation), 0 (no regulation), or +1 (positive regulation);  $w = k_x$  (matching the synthesis  
495 rate constant of  $x$ ), and  $I$  being a random number uniformly distributed in the log range  
496 of 0.01~1.

497 Each of the  $3^5 = 243$  models was simulated with the same set of 10,000 random  
498 parameter sets. With each parameter set, the activity of each node in the Rb-E2f network  
499 was simulated at 50 serum concentrations uniformly distributed in the log range  
500 between 0.01 and 20 (percent of serum, covering the conditions from serum starvation  
501 to saturation). To determine E2f bistability, at each serum concentration, the model with  
502 the initial condition (Table S1) corresponding to the quiescence state was simulated for  
503 1000 model hours to reach the “switch-On” steady state. The “switch-On” steady-state

504 values of individual nodes were then used as the initial condition of the proliferation  
505 state; the model was subsequently simulated for 1000 model hours to reach the “switch-  
506 Off” steady state. Simulation results were analyzed using an “in-house” Perl script,  
507 according to the criteria developed in our previous work [46] to determine E2f  
508 bistability. All simulations were performed using COPASI [63].

### 509 **Modeling phospho-Rb and CycD/Cdk4,6 downregulations**

510 To simulate the CycD/Cdk4,6 downregulation under Cry and Rev-erb agonists, the  
511 CycD/Cdk4,6 term ([CD], Table S1) in the base model of the Rb-E2f bistable switch  
512 [32] was multiplied with a scaling factor ( $\alpha = 0.1\sim 1$ ); phosphorylated Rb ([RP], Table  
513 S1) and total Rb ([R]+[RE]+[RP], Table S1) were accordingly derived by model  
514 simulation. Reversely, given a decrease in relative phospho-Rb under Cry and Rev-erb  
515 agonists as measured in the experiment, the scaling factor  $\alpha$  of [CD] was derived by  
516 simulation and then applied to simulate the E2f serum response. In the time course  
517 simulation of the base model, the 7-hr model time aligned with the 14-hr experimental  
518 time according to phospho-Rb and E2f-GFP dynamics following serum stimulation.  
519 Accordingly, time in all model simulations was adjusted by 7 hours (e.g., the 17-hr  
520 model time was used to simulate serum responses at the 24-hr).

### 521 **Stochastic simulation**

522 Similar to Ref. [64, 65], we built a Langevin-type stochastic differential equation (SDE)  
523 model based on the ODE model described in Table S1.

$$X_i(t + \tau) = X_i(t) + \sum_{j=1}^M v_{ji} a_j[X(t)]\tau + \theta \sum_{j=1}^M v_{ji} (a_j[X(t)]\tau)^{1/2} \gamma + \delta \omega \tau^{1/2}$$

524 where  $X(t) = (X_1(t), \dots, X_n(t))$  is the system state at time  $t$ .  $X_i(t)$  is the molecule  
525 number of species  $i$  ( $i = 1, \dots, n$ ) at time  $t$ . The time evolution of the system is  
526 measured based on the rates  $a_j[X(t)]$  ( $j = 1, \dots, M$ ) with the corresponding change of  
527 molecule number  $i$  described in  $v_{ji}$ . Factors  $\gamma$  and  $\omega$  are two independent and  
528 uncorrelated Gaussian noises. In this equation, the first two terms indicate deterministic  
529 kinetics, the third and fourth terms represent intrinsic and extrinsic noise, respectively.  
530  $\theta$  and  $\delta$  are scaling factors to adjust the levels of intrinsic and extrinsic noise,  
531 respectively ( $\theta=0.45$ ,  $\delta=30$ ). Units of model parameters and species concentrations in  
532 the ODE model (Table S2) were converted to molecule numbers. We considered the  
533 cell reenters the cell cycle with the E2f-ON state, when the E2f molecule number at the

534 24<sup>th</sup> hour after serum stimulation was larger than a cutoff value of 200. All SDEs were  
535 implemented and solved in Matlab.

536

537

538

539

540

541 **ACKNOWLEDGEMENTS**

542 We thank Kotaro Fujimaki, Xiaojun Tian, and Tongli Zhang for critical readings and  
543 comments on the manuscript. This work was supported by grants from the NSF  
544 (#1463137 and 2034210 to GY) and NIH (GM-084905, a T32 fellowship to JSK) of  
545 the U.S.A., and the NSF of China (#31500676 to XW).

546

547

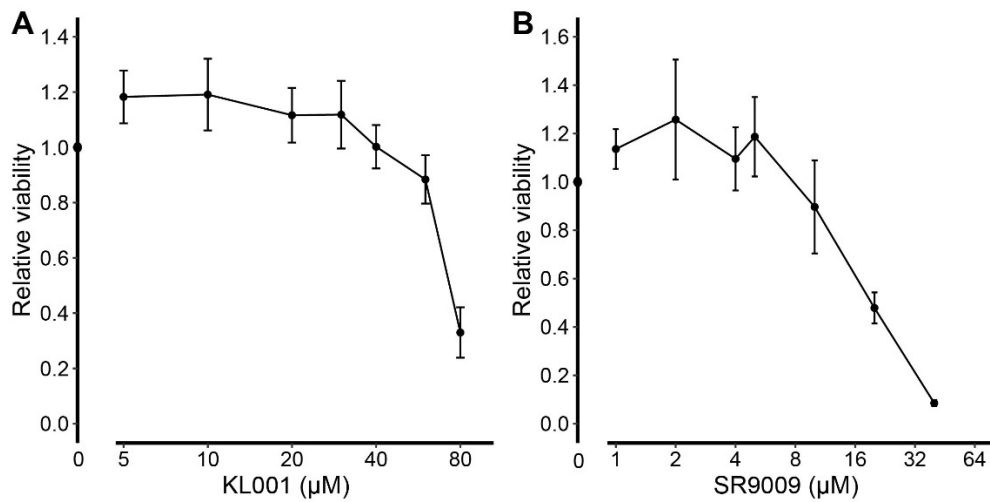
548 **REFERENCES**

- 549 1. Coller HA, Sang L, Roberts JM: **A new description of cellular quiescence.** *PLoS Biol* 2006,  
550 4(3):e83.
- 551 2. Cheung TH, Rando TA: **Molecular regulation of stem cell quiescence.** *Nat Rev Mol Cell Biol*  
552 2013, 14(6):329-340.
- 553 3. Rumman M, Dhawan J, Kassem M: **Concise Review: Quiescence in Adult Stem Cells:  
554 Biological Significance and Relevance to Tissue Regeneration.** *Stem Cells* 2015, 33(10):2903-  
555 2912.
- 556 4. Bouchard-Cannon P, Mendoza-Viveros L, Yuen A, Kaern M, Cheng HY: **The circadian  
557 molecular clock regulates adult hippocampal neurogenesis by controlling the timing of cell-  
558 cycle entry and exit.** *Cell Rep* 2013, 5(4):961-973.
- 559 5. Gengatharan A, Malvaut S, Marymonchuk A, Ghareghani M, Snapyan M, Fischer-Sternjak J,  
560 Ninkovic J, Götz M, Saghatelian A: **Adult neural stem cell activation in mice is regulated by  
561 the day/night cycle and intracellular calcium dynamics.** *Cell* 2021, 184(3):709-722. e713.
- 562 6. Janich P, Pascual G, Merlos-Suarez A, Battle E, Ripperger J, Albrecht U, Cheng HY, Obrietan K,  
563 Di Croce L, Benitah SA: **The circadian molecular clock creates epidermal stem cell  
564 heterogeneity.** *Nature* 2011, 480(7376):209-214.
- 565 7. Panda S, Antoch MP, Miller BH, Su AI, Schook AB, Straume M, Schultz PG, Kay SA, Takahashi  
566 JS, Hogenesch JB: **Coordinated transcription of key pathways in the mouse by the circadian  
567 clock.** *Cell* 2002, 109(3):307-320.
- 568 8. Ueda HR, Chen W, Adachi A, Wakamatsu H, Hayashi S, Takasugi T, Nagano M, Nakahama K,  
569 Suzuki Y, Sugano S *et al*: **A transcription factor response element for gene expression during  
570 circadian night.** *Nature* 2002, 418(6897):534-539.
- 571 9. Storch KF, Lipan O, Leykin I, Viswanathan N, Davis FC, Wong WH, Weitz CJ: **Extensive and  
572 divergent circadian gene expression in liver and heart.** *Nature* 2002, 417(6884):78-83.
- 573 10. Sancar A, Van Gelder RN: **Clocks, cancer, and chronochemotherapy.** *Science* 2021,  
574 371(6524).
- 575 11. Takahashi JS: **Transcriptional architecture of the mammalian circadian clock.** *Nat Rev Genet*  
576 2017, 18(3):164-179.
- 577 12. Hong CI, Zamborszky J, Baek M, Labiscsak L, Ju K, Lee H, Larrondo LF, Goity A, Chong HS,  
578 Belden WJ *et al*: **Circadian rhythms synchronize mitosis in *Neurospora crassa*.** *Proc Natl  
579 Acad Sci U S A* 2014, 111(4):1397-1402.
- 580 13. Yang Q, Pando BF, Dong G, Golden SS, van Oudenaarden A: **Circadian gating of the cell cycle  
581 revealed in single cyanobacterial cells.** *Science* 2010, 327(5972):1522-1526.
- 582 14. Bieler J, Cannavo R, Gustafson K, Gobet C, Gatfield D, Naef F: **Robust synchronization of  
583 coupled circadian and cell cycle oscillators in single mammalian cells.** *Mol Syst Biol* 2014,  
584 10:739.
- 585 15. Feillet C, Krusche P, Tamanini F, Janssens RC, Downey MJ, Martin P, Teboul M, Saito S, Levi  
586 FA, Bretschneider T *et al*: **Phase locking and multiple oscillating attractors for the coupled  
587 mammalian clock and cell cycle.** *Proc Natl Acad Sci U S A* 2014, 111(27):9828-9833.
- 588 16. Liu Z, Selby CP, Yang Y, Lindsey-Boltz LA, Cao X, Eynullazada K, Sancar A: **Circadian regulation  
589 of c-MYC in mice.** *Proc Natl Acad Sci U S A* 2020, 117(35):21609-21617.
- 590 17. Fu L, Pelicano H, Liu J, Huang P, Lee C: **The circadian gene *Period2* plays an important role in  
591 tumor suppression and DNA damage response in vivo.** *Cell* 2002, 111(1):41-50.
- 592 18. Gréchez-Cassiau A, Rayet B, Guillaumond F, Teboul M, Delaunay F: **The circadian clock  
593 component *BMAL1* is a critical regulator of *p21WAF1/CIP1* expression and hepatocyte  
594 proliferation.** *Journal of Biological Chemistry* 2008, 283(8):4535-4542.
- 595 19. Matsuo T, Yamaguchi S, Mitsui S, Emi A, Shimoda F, Okamura H: **Control mechanism of the  
596 circadian clock for timing of cell division in vivo.** *Science* 2003, 302(5643):255-259.
- 597 20. Sahar S, Sassone-Corsi P: **Metabolism and cancer: the circadian clock connection.** *Nat Rev  
598 Cancer* 2009, 9(12):886-896.
- 599 21. Kwon JS, Everetts NJ, Wang X, Wang W, Della Croce K, Xing J, Yao G: **Controlling Depth of  
600 Cellular Quiescence by an Rb-E2F Network Switch.** *Cell Rep* 2017, 20(13):3223-3235.
- 601 22. Brooks RF, Richmond FN, Riddle PN, Richmond KM: **Apparent heterogeneity in the response  
602 of quiescent swiss 3T3 cells to serum growth factors: implications for the transition**

- 603 **probability model and parallels with "cellular senescence" and "competence".** *J Cell Physiol*  
604 1984, **121**(2):341-350.
- 605 23. Fujimaki K, Li R, Chen H, Della Croce K, Zhang HH, Xing J, Bai F, Yao G: **Graded regulation of**  
606 **cellular quiescence depth between proliferation and senescence by a lysosomal dimmer**  
607 **switch.** *Proceedings of the National Academy of Sciences* 2019, **116**(45):22624-22634.
- 608 24. Augenlicht LH, Baserga R: **Changes in the G0 state of WI-38 fibroblasts at different times**  
609 **after confluence.** *Exp Cell Res* 1974, **89**(2):255-262.
- 610 25. Bucher NL: **Regeneration of Mammalian Liver.** *Int Rev Cytol* 1963, **15**:245-300.
- 611 26. Roth GS, Adelman RC: **Age-dependent regulation of mammalian DNA synthesis and cell**  
612 **division in vivo by glucocorticoids.** *Exp Gerontol* 1974, **9**(1):27-31.
- 613 27. Yanez I, O'Farrell M: **Variation in the length of the lag phase following serum restimulation**  
614 **of mouse 3T3 cells.** *Cell Biol Int Rep* 1989, **13**(5):453-462.
- 615 28. Rodgers JT, King KY, Brett JO, Cromie MJ, Charville GW, Maguire KK, Brunson C, Mastey N, Liu  
616 L, Tsai CR *et al*: **mTORC1 controls the adaptive transition of quiescent stem cells from G0 to**  
617 **G(Alert).** *Nature* 2014, **510**(7505):393-396.
- 618 29. Llorens-Bobadilla E, Zhao S, Baser A, Saiz-Castro G, Zwadlo K, Martin-Villalba A: **Single-Cell**  
619 **Transcriptomics Reveals a Population of Dormant Neural Stem Cells that Become Activated**  
620 **upon Brain Injury.** *Cell Stem Cell* 2015, **17**(3):329-340.
- 621 30. Rodgers JT, Schroeder MD, Ma C, Rando TA: **HGFA is an injury-regulated systemic factor**  
622 **that induces the transition of stem cells into GAlert.** *Cell reports* 2017, **19**(3):479-486.
- 623 31. Lee G, Espirito Santo AI, Zwingenberger S, Cai L, Vogl T, Feldmann M, Horwood NJ, Chan JK,  
624 Nanchahal J: **Fully reduced HMGB1 accelerates the regeneration of multiple tissues by**  
625 **transitioning stem cells to GAlert.** *Proc Natl Acad Sci U S A* 2018, **115**(19):E4463-E4472.
- 626 32. Yao G, Lee TJ, Mori S, Nevins JR, You L: **A bistable Rb-E2F switch underlies the restriction**  
627 **point.** *Nat Cell Biol* 2008, **10**(4):476-482.
- 628 33. Wang X, Fujimaki K, Mitchell GC, Kwon JS, Della Croce K, Langsdorf C, Zhang HH, Yao G: **Exit**  
629 **from quiescence displays a memory of cell growth and division.** *Nat Commun* 2017,  
630 **8**(1):321.
- 631 34. Wu L, Timmers C, Maiti B, Saavedra HI, Sang L, Chong GT, Nuckolls F, Giangrande P, Wright  
632 FA, Field SJ *et al*: **The E2F1-3 transcription factors are essential for cellular proliferation.**  
633 *Nature* 2001, **414**(6862):457-462.
- 634 35. Johnson DG, Schwarz JK, Cress WD, Nevins JR: **Expression of transcription factor E2F1**  
635 **induces quiescent cells to enter S phase.** *Nature* 1993, **365**(6444):349-352.
- 636 36. Yao G: **Modelling mammalian cellular quiescence.** *Interface Focus* 2014, **4**(3):20130074.
- 637 37. Cappell SD, Chung M, Jaimovich A, Spencer SL, Meyer T: **Irreversible APCdh1 inactivation**  
638 **underlies the point of no return for cell-cycle entry.** *Cell* 2016, **166**(1):167-180.
- 639 38. Cappell SD, Mark KG, Garbett D, Pack LR, Rape M, Meyer T: **EMI1 switches from being a**  
640 **substrate to an inhibitor of APC/C CDH1 to start the cell cycle.** *Nature* 2018, **558**(7709):313-  
641 317.
- 642 39. Leung JY, Ehmann GL, Giangrande PH, Nevins JR: **A role for Myc in facilitating transcription**  
643 **activation by E2F1.** *Oncogene* 2008, **27**(30):4172-4179.
- 644 40. Hirota T, Lee JW, St John PC, Sawa M, Iwaisako K, Noguchi T, Pongsawakul PY, Sonntag T,  
645 Welsh DK, Brenner DA *et al*: **Identification of small molecule activators of cryptochrome.**  
646 *Science* 2012, **337**(6098):1094-1097.
- 647 41. Calzone L, Gelay A, Zinovyev A, Radvanyi F, Barillot E: **A comprehensive modular map of**  
648 **molecular interactions in RB/E2F pathway.** *Mol Syst Biol* 2008, **4**:173.
- 649 42. Sears RC, Nevins JR: **Signaling networks that link cell proliferation and cell fate.** *Journal of*  
650 *Biological Chemistry* 2002, **277**(14):11617-11620.
- 651 43. Attwooll C, Lazzarini Denchi E, Helin K: **The E2F family: specific functions and overlapping**  
652 **interests.** *EMBO J* 2004, **23**(24):4709-4716.
- 653 44. Frolov MV, Dyson NJ: **Molecular mechanisms of E2F-dependent activation and pRB-**  
654 **mediated repression.** *J Cell Sci* 2004, **117**(Pt 11):2173-2181.
- 655 45. Weinberg RA: **The retinoblastoma protein and cell cycle control.** *Cell* 1995, **81**(3):323-330.
- 656 46. Yao G, Tan C, West M, Nevins JR, You L: **Origin of bistability underlying mammalian cell**  
657 **cycle entry.** *Mol Syst Biol* 2011, **7**:485.
- 658 47. Ma W, Lai L, Ouyang Q, Tang C: **Robustness and modular design of the Drosophila segment**  
659 **polarity network.** *Mol Syst Biol* 2006, **2**:70.

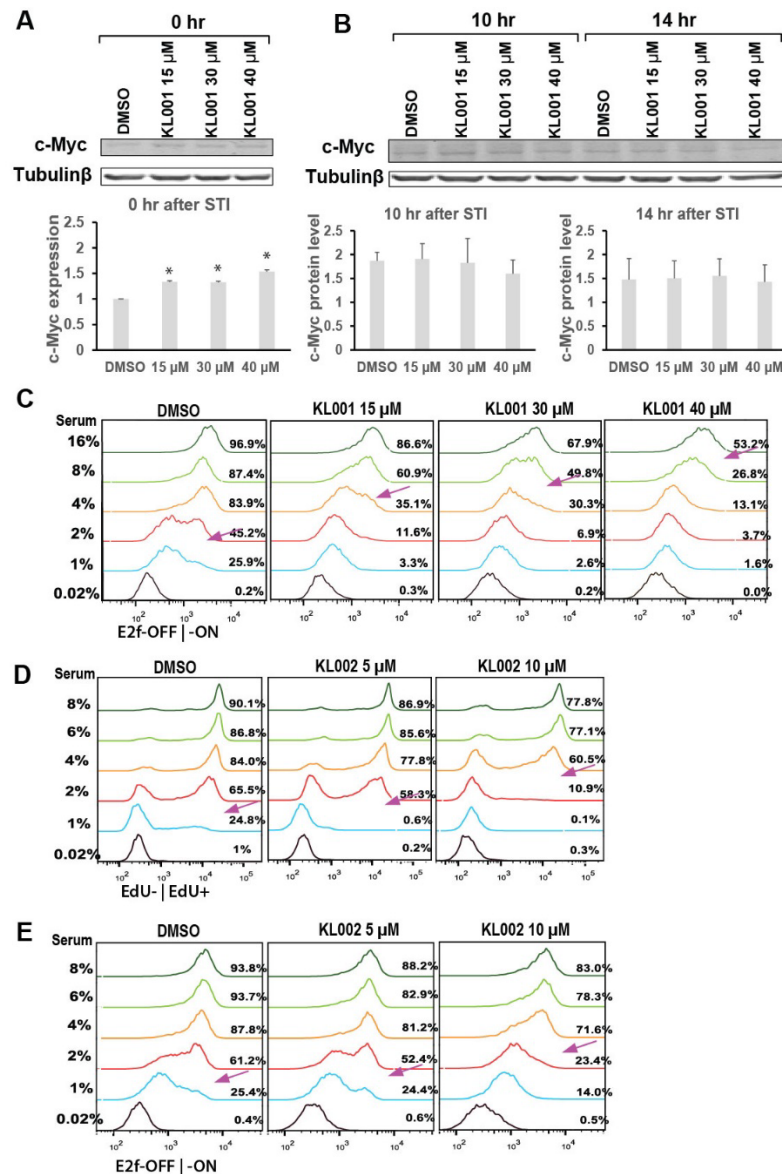


- 660 48. Ma W, Trusina A, El-Samad H, Lim WA, Tang C: **Defining network topologies that can**  
661 **achieve biochemical adaptation.** *Cell* 2009, **138**(4):760-773.
- 662 49. Arora M, Moser J, Phadke H, Basha AA, Spencer SL: **Endogenous Replication Stress in**  
663 **Mother Cells Leads to Quiescence of Daughter Cells.** *Cell Rep* 2017, **19**(7):1351-1364.
- 664 50. Barr AR, Cooper S, Heldt FS, Butera F, Stoy H, Mansfeld J, Novak B, Bakal C: **DNA damage**  
665 **during S-phase mediates the proliferation-quiescence decision in the subsequent G1 via**  
666 **p21 expression.** *Nat Commun* 2017, **8**:14728.
- 667 51. Laurenti E, Frelin C, Xie S, Ferrari R, Dunant CF, Zandi S, Neumann A, Plumb I, Doulatov S,  
668 Chen J *et al*: **CDK6 levels regulate quiescence exit in human hematopoietic stem cells.** *Cell*  
669 *Stem Cell* 2015, **16**(3):302-313.
- 670 52. Yang HW, Chung M, Kudo T, Meyer T: **Competing memories of mitogen and p53 signalling**  
671 **control cell-cycle entry.** *Nature* 2017, **549**(7672):404-408.
- 672 53. Min M, Rong Y, Tian C, Spencer SL: **Temporal integration of mitogen history in mother cells**  
673 **controls proliferation of daughter cells.** *Science* 2020, **368**(6496):1261-1265.
- 674 54. Narasimha AM, Kaulich M, Shapiro GS, Choi YJ, Sicinski P, Dowdy SF: **Cyclin D activates the**  
675 **Rb tumor suppressor by mono-phosphorylation.** *Elife* 2014, **3**.
- 676 55. Pennycook BR, Barr AR: **Restriction point regulation at the crossroads between quiescence**  
677 **and cell proliferation.** *FEBS letters* 2020, **594**(13):2046-2060.
- 678 56. Schwarz C, Johnson A, Kõivomägi M, Zatulovskiy E, Kravitz CJ, Doncic A, Skotheim JM: **A**  
679 **precise Cdk activity threshold determines passage through the restriction point.** *Molecular*  
680 *cell* 2018, **69**(2):253-264. e255.
- 681 57. Stallaert W, Kedziora KM, Chao HX, Purvis JE: **Bistable switches as integrators and actuators**  
682 **during cell cycle progression.** *FEBS letters* 2019, **593**(20):2805-2816.
- 683 58. Brooks RF: **Cell cycle commitment and the origins of cell cycle variability.** *Frontiers in Cell*  
684 *and Developmental Biology* 2021, **9**:1891.
- 685 59. Matson JP, Cook JG: **Cell cycle proliferation decisions: the impact of single cell analyses.**  
686 *FEBS J* 2017, **284**(3):362-375.
- 687 60. Novák B, Tyson JJ: **Mechanisms of signalling-memory governing progression through the**  
688 **eukaryotic cell cycle.** *Current Opinion in Cell Biology* 2021, **69**:7-16.
- 689 61. Goldbeter A, Koshland DE, Jr.: **An amplified sensitivity arising from covalent modification in**  
690 **biological systems.** *Proc Natl Acad Sci U S A* 1981, **78**(11):6840-6844.
- 691 62. Overton KW, Spencer SL, Noderer WL, Meyer T, Wang CL: **Basal p21 controls population**  
692 **heterogeneity in cycling and quiescent cell cycle states.** *Proc Natl Acad Sci U S A* 2014,  
693 **111**(41):E4386-4393.
- 694 63. Hoops S, Sahle S, Gauges R, Lee C, Pahle J, Simus N, Singhal M, Xu L, Mendes P, Kummer U:  
695 **COPASI: a COMplex PATHway Simulator.** *Bioinformatics* 2006, **22**(24):3067-3074.
- 696 64. Lee TJ, Yao G, Bennett DC, Nevins JR, You L: **Stochastic E2F activation and reconciliation of**  
697 **phenomenological cell-cycle models.** *PLoS Biol* 2010, **8**(9).
- 698 65. Gillespie DT: **The chemical Langevin equation.** *The Journal of Chemical Physics* 2000,  
699 **113**(1):297-306.
- 700 66. Dengler WA, Schulte J, Berger DP, Mertelsmann R, Fiebig HH: **Development of a propidium**  
701 **iodide fluorescence assay for proliferation and cytotoxicity assays.** *Anticancer Drugs* 1995,  
702 **6**(4):522-532.
- 703 67. Phillips NE, Hugues A, Yeung J, Durandau E, Nicolas D, Naef F: **The circadian oscillator**  
704 **analysed at the single-transcript level.** *Molecular systems biology* 2021, **17**(3):e10135.
- 705
- 706



707  
708  
709  
710  
711  
712  
713  
714

**Figure S1. Cytotoxicity of Cry and Rev-erb agonists in REF52/E23 cells.** Cells were treated with Cry agonist KL001 (A) and Rev-erb agonist SR9009 (B), respectively, at the indicated concentrations for 48 hours (concentration = 0 being the DMSO vehicle control). Relative viability (y-axis) refers to the ratio of the live cell count in a treated sample over that in the DMSO control. Live cell count was determined by the PI fluorescence assay as previously described [66]. Error bar, SD (n = 3).



715

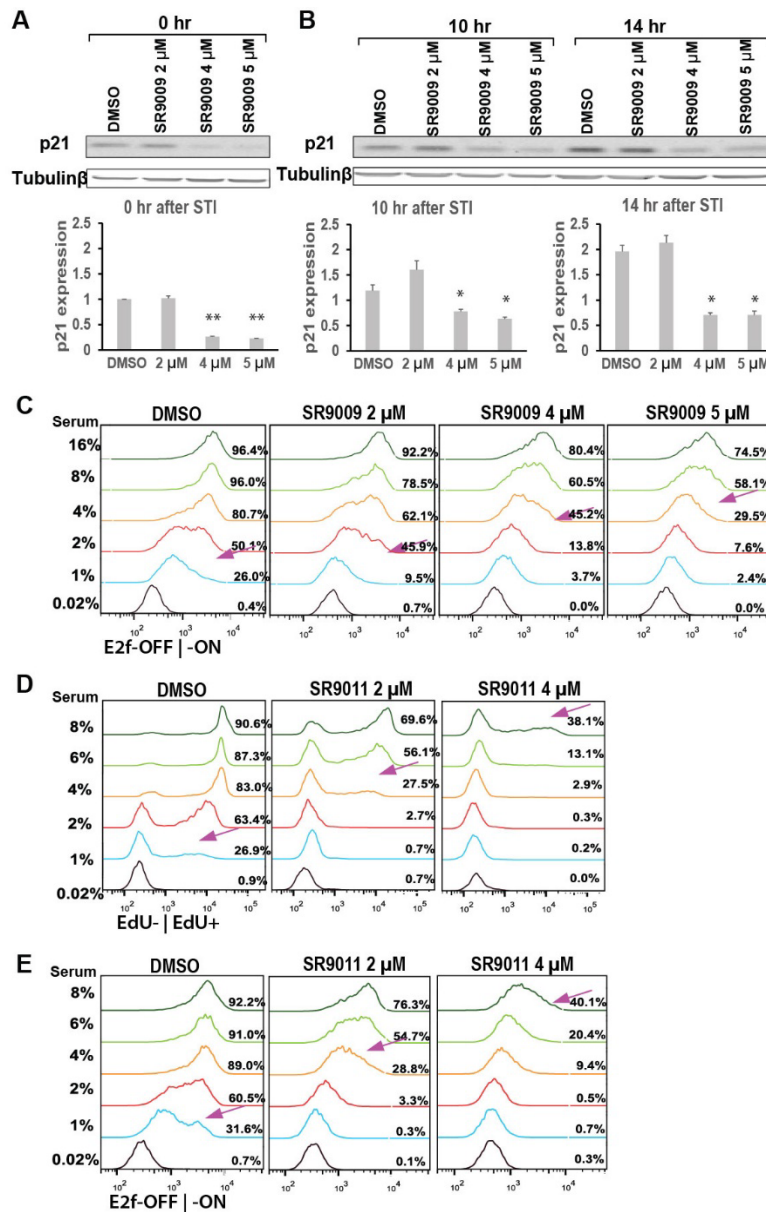
716 **Figure S2. Cry agonists induce cells into deeper quiescence.**

717 (A-B) Effect of Cry agonist KL001 on Myc protein level. Quiescent cells were serum (4%)  
 718 stimulated following the STI.3dq/agonist protocol in the presence of KL001 at the indicated  
 719 concentrations. The protein levels of c-Myc were assessed by Western blot at (A) the 0 hr, i.e., in  
 720 quiescent cells, and (B) the 10- and 14-hr time points after serum stimulation (STI). Error bar, SEM  
 721 (n = 2). \*p < 0.05.

722 (C) Effect of KL001 on quiescence depth. Quiescent cells were serum stimulated following the  
 723 STI.3dq/agonist protocol. Serum and KL001 concentrations are as indicated. The percentages of  
 724 cells with E2f-ON at the 24-hr after serum stimulation are indicated to the right of individual  
 725 histograms. Arrows indicate the approximate serum concentrations leading to E2f-ON% = 45%.

726 (D-E) Effect of Cry agonist KL002 on quiescence depth. Quiescent cells were serum stimulated  
 727 following the STI.3dq/agonist protocol. Serum and KL002 concentrations are as indicated. The  
 728 EdU+% at the 30-hr (D) and the E2f-ON% at the 24-hr (E) after serum stimulation are indicated to  
 729 the right of individual histograms. Arrows indicate the approximate serum concentrations leading  
 730 to EdU+% (D) and E2f-ON% (E) = 45%, respectively.

731



732

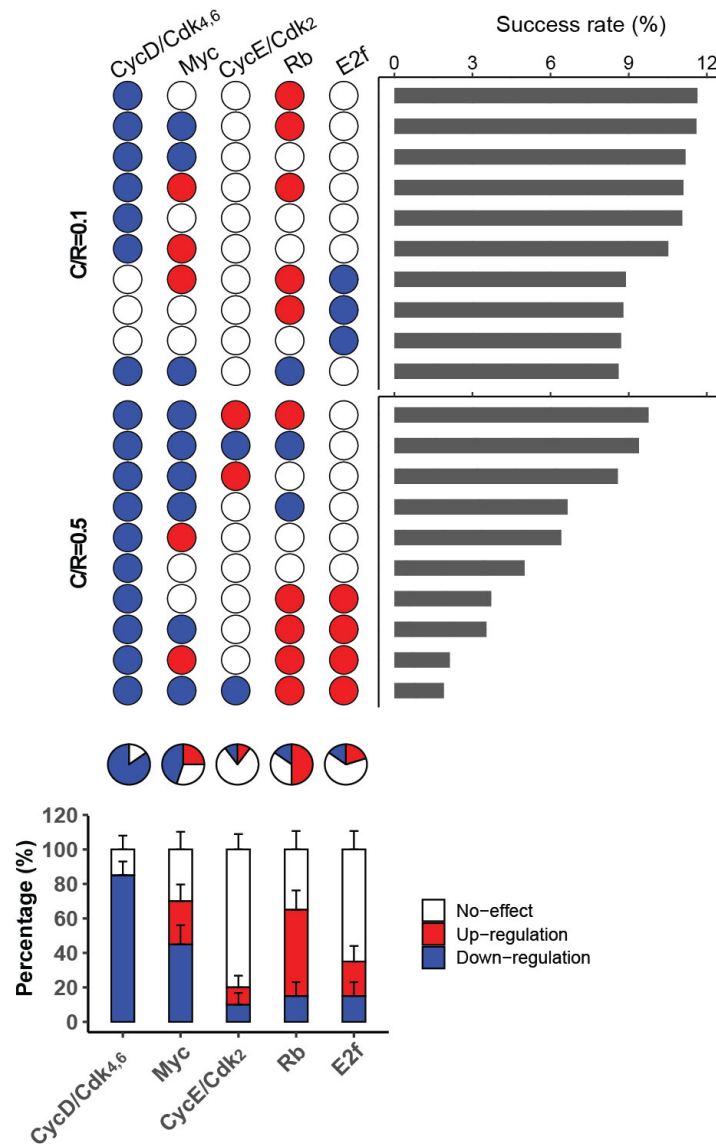
733 **Figure S3. Rev-erb agonists induce cells into deeper quiescence.**

734 (A-B) Effect of Rev-erb agonist SR9009 on p21 protein level. Quiescent cells were serum (4%)  
 735 stimulated following the STI.3dq/agonist protocol in the presence of SR9009 at the indicated  
 736 concentrations. The protein levels of p21 were measured by Western blot at (A) the 0 hr (i.e., in  
 737 quiescent cells), and (B) the 10- and 14-hr after serum stimulation (STI). Error bar, SEM (n = 2).  
 738 \*p < 0.05.

739 (C) Effect of SR9009 on quiescence depth. Quiescent cells were serum stimulated following the  
 740 STI.3dq/agonist protocol. Serum and SR9009 concentrations are as indicated. E2f-ON% at the 24-  
 741 hr after serum stimulation are indicated to the right of individual histograms. Arrows indicate the  
 742 approximate serum concentrations leading to E2f-ON% = 45%.

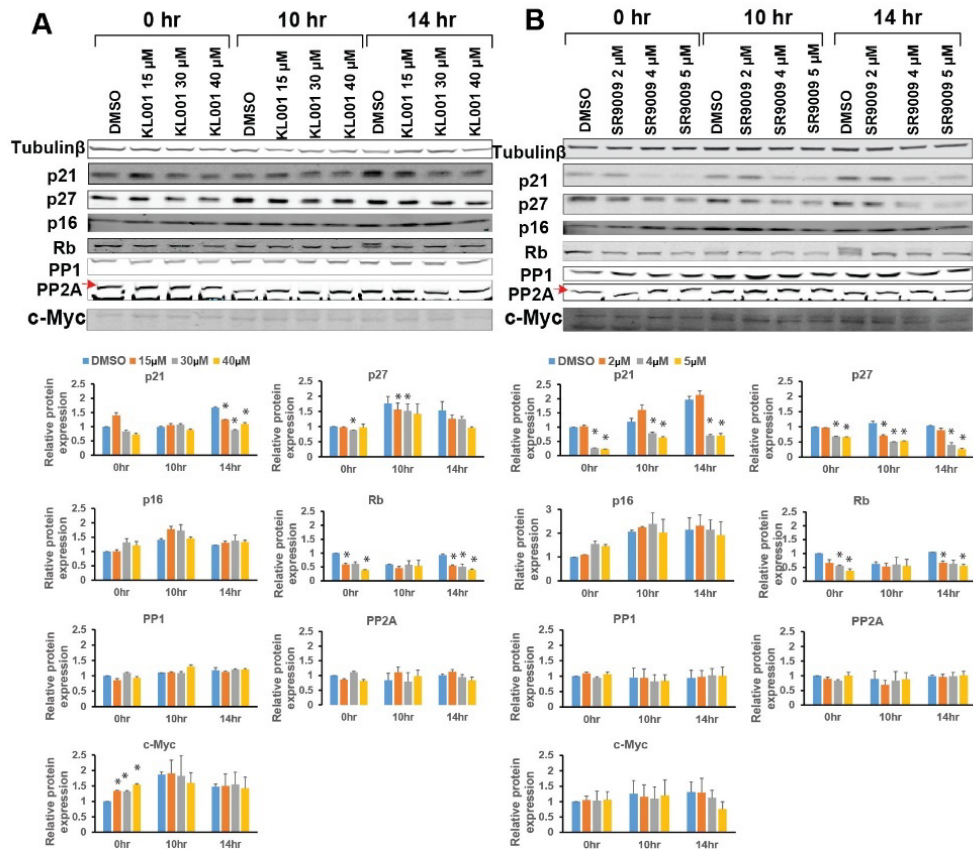
743 (D-E) Effect of Rev-erb agonist SR9011 on quiescence depth. Quiescent cells were stimulated  
 744 following the STI.3dq/agonist protocol. Serum and SR9011 concentrations are as indicated. The  
 745 EdU+% at the 30-hr (D) and the E2f-ON% at the 24-hr (E) after serum stimulation are indicated to  
 746 the right of individual histograms. Arrows indicate the approximate serum concentrations leading  
 747 to EdU+% (D) and E2f-ON% (E) = 45%, respectively.

748



749  
750  
751  
752  
753  
754  
755

**Figure S4. Link features of the 10 top-ranked models at each C/R level.** (Top) The top 10 models at  $C/R = 0.1$  and  $0.5$ , respectively. The link features in each model are shown according to the upregulation (red), downregulation (blue), or no-effect (white) of the indicated target node by  $C/R$ . (Middle) Pie chart of the percentage of each link feature at the indicated target node among the combined 20 models (top). (Bottom) The average percentage of each link feature at the indicated target node between the two model groups ( $C/R = 0.1$  and  $0.5$ , respectively, top). Error bar, SD.



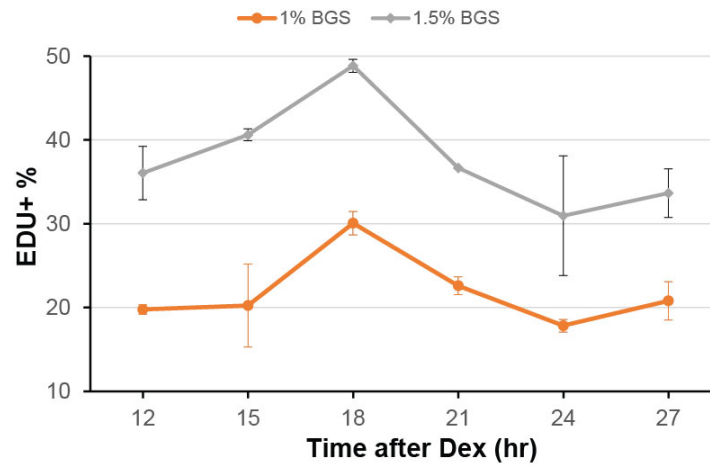
756

757 **Figure S5. Western blot analysis of multiple Rb-E2f network proteins in response to Cry and**  
 758 **Rev-erb agonists.**

759 The responses of indicated Rb-E2f network proteins to Cry agonist KL001 (A) and Rev-erb agonist  
 760 SR9009 (B) at the indicated concentrations were measured following the STI.3dq/agonist protocol.  
 761 Protein levels were measured by Western blot in quiescence (0 hr) and during cell cycle entry (10  
 762 and 14 hr after stimulated with 4% serum) and normalized to the 0-hr DMSO control. Error bar,  
 763 SEM (n=2); \*p < 0.05.  
 764



765  
766  
767



768

769 **Figure S6. Circadian changes of quiescence depth.**

770 Quiescent (2-day serum-starved) cells were circadian-synchronized with dexamethasone (Dex, 100  
771 nM) treatment for 2 hours followed by 12 hours of stabilization time (as in [67]). Cells were  
772 subsequently, and every 3 hours afterward, stimulated with serum (1% and 1.5%, respectively) for  
773 30 hours, followed by the measurement of EdU+%. Error bar, SEM ( $n \geq 2$ ).



- 774 **Table S1.** Rb-E2f bistable switch model with circadian regulation.
- 775 **Table S2.** Model parameters.
- 776 **Table S3.** Ranking for the top 10 topologies at the low level of C/R (= 0.1).
- 777 **Table S4.** Ranking for the top 10 topologies at the high level of C/R (= 0.5).
- 778 **Table S5.** Estimation of CycD/Cdk4,6 activity under KL001 and SR9009 treatments.

**Table S1.** The Rb-E2f bistable switch model with circadian regulation (adapted from Ref. [1]).

$\frac{d[M]}{dt} = \frac{k_M[S]}{K_S + [S]} + \frac{m_1 \cdot w_1 \cdot [CR]}{I_1 + [CR]} - d_M[M]$
$\frac{d[CD]}{dt} = \frac{k_{CD}[M]}{K_M + [M]} + \frac{k_{CDS}[S]}{K_S + [S]} + \frac{m_2 \cdot w_2 \cdot [CR]}{I_2 + [CR]} - d_{CD}[CD]$
$\frac{d[R]}{dt} = k_R + \frac{m_3 \cdot w_3 \cdot [CR]}{I_3 + [CR]} + \frac{k_{DP}[RP]}{K_{RP} + [RP]} - k_{RE}[R][E] - \frac{k_{P1}[CD][R]}{K_{CD} + [R]} - \frac{k_{P2}[CE][R]}{K_{CE} + [R]} - d_R[R]$
$\frac{d[CE]}{dt} = \frac{k_{CE}[E]}{K_E + [E]} + \frac{m_4 \cdot w_4 \cdot [CR]}{I_4 + [CR]} - d_{CE}[CE]$
$\frac{d[E]}{dt} = k_E \left( \frac{[M]}{K_M + [M]} \right) \left( \frac{[E]}{K_E + [E]} \right) + \frac{k_b[M]}{K_M + [M]} + \frac{m_5 \cdot w_5 \cdot [CR]}{I_5 + [CR]} + \frac{k_{P1}[CD][RE]}{K_{CD} + [RE]} + \frac{k_{P2}[CE][RE]}{K_{CE} + [RE]} - k_{RE}[R][E] - d_E[E]$
$\frac{d[RP]}{dt} = \frac{k_{P1}[CD][R]}{K_{CD} + [R]} + \frac{k_{P2}[CE][R]}{K_{CE} + [R]} + \frac{k_{P1}[CD][RE]}{K_{CD} + [RE]} + \frac{k_{P2}[CE][RE]}{K_{CE} + [RE]} - \frac{k_{DP}[RP]}{K_{RP} + [RP]} - d_{RP}[RP]$
$\frac{d[RE]}{dt} = k_{RE}[R][E] - \frac{k_{P1}[CD][RE]}{K_{CD} + [RE]} - \frac{k_{P2}[CE][RE]}{K_{CE} + [RE]} - d_{RE}[RE]$

Variables:

*S*: serum concentration

*M*: Myc

*E*: E2F

*CD*: Cyclin D/Cdk4,6

*CE*: Cyclin E/Cdk2

*R*: Rb family proteins

*RP*: Phosphorylated Rb

*RE*: Rb-E2F complex

*CR*: Cry or Rev-erb

Initial condition:

$[M] = [E] = [CD] = [CE] = [R] = [RP] = 0$  nM,  $[RE] = 0.55$  nM,  $[CR] = 0.1$  or  $0.5$  nM.

Note: Model parameters are adapted from [1] and defined in Table S2 (including newly added parameters  $m_{1-5}$ ,  $w_{1-5}$ , and  $I_{1-5}$ ).

**Table S2.** Model parameters (adapted from Ref. [1])

Symbol	Values	Description
$k_M$	1.0 nM hr <sup>-1</sup>	Rate constant of Myc synthesis driven by growth factors
$k_E$	0.4 nM hr <sup>-1</sup>	Rate constant of E2F synthesis driven by Myc and E2F
$k_b$	0.003 nM hr <sup>-1</sup>	Rate constant of E2F synthesis driven by Myc alone
$k_{CD}$	0.03 nM hr <sup>-1</sup>	Rate constant of CycD synthesis driven by Myc
$k_{CDS}$	0.45 nM hr <sup>-1</sup>	Rate constant of CycD synthesis driven by growth factors
$k_{CE}$	0.35 nM hr <sup>-1</sup>	Rate constant of CycE synthesis driven by E2F
$k_R$	0.18 nM hr <sup>-1</sup>	Rate constant of Rb constitutive synthesis
$k_{P1}$	18 hr <sup>-1</sup>	Phosphorylation rate constant of Rb by CycD/Cdk4,6
$k_{P2}$	18 hr <sup>-1</sup>	Phosphorylation rate constant of Rb by CycE/Cdk2
$k_{DP}$	3.6 nM hr <sup>-1</sup>	Dephosphorylation rate constant of Rb by phosphatases
$k_{RE}$	180 nM <sup>-1</sup> hr <sup>-1</sup>	Association rate constant of Rb and E2F
$K_S$	0.5 nM	Michaelis-Menten parameter for CycD and Myc synthesis by growth factors
$K_E$	0.15 nM	Michaelis-Menten parameter for CycE and E2F synthesis by E2F
$K_M$	0.15 nM	Michaelis-Menten parameter for CycD and E2F synthesis by Myc
$K_{RP}$	0.01 nM	Michaelis-Menten parameter for Rb dephosphorylation
$K_{CD}$	0.92 nM	Michaelis-Menten parameter for Rb phosphorylation by CycD/Cdk4,6
$K_{CE}$	0.92 nM	Michaelis-Menten parameter for Rb phosphorylation by CycE/Cdk2
$d_M$	0.7 hr <sup>-1</sup>	Degradation rate constant of Myc
$d_E$	0.25 hr <sup>-1</sup>	Degradation rate constant of E2F
$d_{CD}$	1.5 hr <sup>-1</sup>	Degradation rate constant of CycD
$d_{CE}$	1.5 hr <sup>-1</sup>	Degradation rate constant of CycE
$d_R$	0.06 hr <sup>-1</sup>	Degradation rate constant of Rb
$d_{RP}$	0.06 hr <sup>-1</sup>	Degradation rate constant of phosphorylated Rb
$d_{RE}$	0.03 hr <sup>-1</sup>	Degradation rate constant of Rb-E2F complex
$m_1$	0, -1, or +1	CR activate, inhibit, or have no effect on $M$
$m_2$	0, -1, or +1	CR activate, inhibit, or have no effect on $CD$
$m_3$	0, -1, or +1	CR activate, inhibit, or have no effect on $R$
$m_4$	0, -1, or +1	CR activate, inhibit, or have no effect on $CE$
$m_5$	0, -1, or +1	CR activate, inhibit, or have no effect on $E$
$w_1$	1.0 nM hr <sup>-1</sup>	Rate constant of CR effect on $M$ (matching the $k_m$ value)
$w_2$	0.45 nM hr <sup>-1</sup>	Rate constant of CR effect on $CD$ (matching the $k_{CDS}$ value)
$w_3$	0.18 nM hr <sup>-1</sup>	Rate constant of CR effect on $R$ (matching the $k_R$ value)
$w_4$	0.35 nM hr <sup>-1</sup>	Rate constant of CR effect on $CE$ (matching the $k_{CE}$ value)
$w_5$	0.4 nM hr <sup>-1</sup>	Rate constant of CR effect on $E$ (matching the $k_E$ value)
$I_1$	0.01 ~ 1 nM	Random Michaelis-Menten parameter for CR effect on $M$
$I_2$	0.01 ~ 1 nM	Random Michaelis-Menten parameter for CR effect on $CD$
$I_3$	0.01 ~ 1 nM	Random Michaelis-Menten parameter for CR effect on $R$
$I_4$	0.01 ~ 1 nM	Random Michaelis-Menten parameter for CR effect on $CE$
$I_5$	0.01 ~ 1 nM	Random Michaelis-Menten parameter for CR effect on $E$

**Table S3.** Ranking of the top 10 topologies at the low level of C/R (= 0.1).

Topology	1250 Sim	2500 Sim	3750 Sim	5000 Sim	6250 Sim	7500 Sim	8750 Sim	10,000 Sim
#64	1	1	2	2	1	1	2	1
#226	2	2	1	1	2	2	1	2
#217	4	4	3	3	3	5	3	3
#145	3	5	5	5	5	3	4	4
#55	5	3	4	4	4	4	5	5
#136	6	6	6	6	6	6	6	6
#93	7	7	8	9	7	7	7	7
#12	8	9	9	11	9	8	8	8
#3	10	8	7	7	8	9	9	9
#235	9	13	11	8	10	10	10	10

A total of 10,000 model simulations (Sim) were evenly divided into 8 bins (1250 Sim in each bin). The ranking of each topology (model number shown in the 1<sup>st</sup> column) was updated after each bin addition (i.e., after 1250, 2500, ..., 10,000 Sim).

**Table S4.** Ranking of the top 10 topologies at the high level of C/R (= 0.5).

Topology	1250 Sim	2500 Sim	3750 Sim	5000 Sim	6250 Sim	7500 Sim	8750 Sim	10,000 Sim
#229	2	2	1	1	1	1	1	1
#241	1	1	2	2	2	2	2	2
#220	3	3	3	3	3	3	3	3
#235	5	5	5	5	5	4	4	4
#136	4	4	4	4	4	5	5	5
#55	6	6	6	6	6	6	6	6
#65	8	7	7	7	7	7	7	7
#227	7	8	8	8	8	8	8	8
#146	10	9	10	9	9	9	9	9
#233	9	10	11	10	10	10	10	10

See Table S3 legend for detail.

**Table S5.** Estimation of CycD/Cdk4,6 activity under KL001 and SR9009 treatments.

<b>KL001</b>													
treatment (rep 1)	CycD1	CycD3	Cdk4	Cdk6	p21	p27	p16	JA (w/o adj. exp)	JA' (w/ adj. exp)	Mean JA'	sd	normalized JA'	sd
DMSO	3.59	0.90	1.22	2.29	1.33	1.91	1.33	2.58	4.66	4.96	0.43	<b>1.00</b>	0.00
KL001 15uM	3.15	0.71	1.14	1.43	1.13	1.58	1.53	1.76	3.99	3.88	0.16	<b>0.78</b>	0.07
KL001 30uM	2.53	0.53	1.18	1.14	1.01	1.54	1.56	1.30	3.38	3.51	0.18	<b>0.71</b>	0.07
KL001 40uM	1.67	0.47	0.90	0.47	0.99	1.37	1.45	0.57	1.92	1.60	0.45	<b>0.32</b>	0.10
treatment (rep 2)	CycD1	CycD3	CDK4	CDK6	p21	p27	p16	JA (w/o adj. exp)	JA' (w/ adj. exp)				
DMSO	2.61	1.23	1.42	2.29	1.34	1.39	1.29	2.66	5.26				
KL001 15uM	1.94	0.95	1.32	1.72	1.18	1.23	1.55	1.66	3.77				
KL001 30uM	1.30	0.94	1.42	1.25	0.94	1.21	1.55	1.21	3.63				
KL001 40uM	0.78	0.75	0.67	0.48	0.99	1.00	1.33	0.40	1.28				
<b>SR9009</b>													
treatment (rep 1)	CycD1	CycD3	Cdk4	Cdk6	p21	p27	p16	JA (w/o adj. exp)	JA' (w/ adj. exp)	Mean JA'	sd	normalized JA'	sd
DMSO	4.10	1.27	1.53	1.59	1.45	1.11	2.39	2.53	6.03	5.77	0.37	<b>1.00</b>	0.00
SR9009 2uM	4.65	0.97	1.12	1.15	1.71	0.85	2.52	1.89	4.17	3.95	0.30	<b>0.69</b>	0.07
SR9009 4uM	0.47	0.37	0.56	0.44	0.70	0.42	2.70	0.16	0.52	0.50	0.02	<b>0.09</b>	0.01
SR9009 5uM	0.22	0.31	0.52	0.32	0.61	0.38	2.54	0.09	0.34	0.31	0.05	<b>0.06</b>	0.01
treatment (rep 2)	CycD1	CycD3	CDK4	CDK6	p21	p27	p16	JA (w/o adj. exp)	JA' (w/ adj. exp)				
DMSO	3.83	1.20	1.46	1.36	1.69	1.06	1.82	2.33	5.50				
SR9009 2uM	4.45	0.91	1.08	0.92	2.03	0.74	2.03	1.68	3.74				
SR9009 4uM	0.49	0.28	0.52	0.26	0.78	0.49	1.84	0.14	0.49				
SR9009 5uM	0.20	0.16	0.49	0.21	0.72	0.42	1.41	0.07	0.27				
<i>Gene expression (estimated from Ref [2])</i>													
	CycD1	CycD3	Cdk4	Cdk6	p21	p27	p16						
relative expression	0.64	1.00	0.89	0.03	0.30	0.10	0.15						
sd	0.00013	0	0.00023	2.2E-05	0.00012	2.4E-05	8.1E-05						

The protein levels of CycD1, CycD3, Cdk4, Cdk6, p21, p27, and p16 were derived from Western blot as in Fig. 3 and S5 and averaged over 10 and 14 hr in each of the two replicates (rep 1 and 2). The joint activity (JA) of CycD/Cdk4,6 was assumed to be positively proportional to the combined levels of CycD and Cdk4,6 components and negatively proportional to the combined level of CKI components,  $JA = (CycD1+CycD3)(Cdk4+Cdk6)/(p16+p21+p27)$ . Next, JA was adjusted (JA') according to the relative gene expression level of each component (estimated from Ref. [2] based on the RNA-seq data in growing REF/E23 cells). The mean JA' value was obtained by averaging over rep 1 and 2 at each treatment condition and subsequently normalized to the DMSO control. (sd, standard deviation).

## Supplementary References

1. Yao, G., et al., *A bistable Rb-E2F switch underlies the restriction point*. Nat Cell Biol, 2008. **10**(4): p. 476-82.
2. Fujimaki, K., et al., *Graded regulation of cellular quiescence depth between proliferation and senescence by a lysosomal dimmer switch*. Proceedings of the National Academy of Sciences, 2019. **116**(45): p. 22624-22634.